ISSN 1070-3284, Russian Journal of Coordination Chemistry, 2014, Vol. 40, No. 6, pp. 371–378. © Pleiades Publishing, Ltd., 2014.

Synthesis, Characterization, and Antibacterial Activity of Two Zinc(II) Complexes with Schiff Bases Derived from Rimantadine[1]

X. D. Jin[a, *], C. Xu[a], X. Y. Yin[a], H. B. Wang[a], Z. Y. Zou[b], D. L. Liu[a], C. H. Ge[a], X. H. Chang[a], and Y. H. Jin[c]

[a] *College of Chemistry, Liaoning University, Shenyang, 110036 P.R. China*
[b] *Department of Life Science, Liaoning University, Shenyang, 110036 P.R. China*
[c] *Liaoning Provincial Institute of Measurement, Shenyang, 110036 P.R. China*
**e-mail: jinxudong@yahoo.com*

Received September 6, 2013

Abstract—The reactions of zinc(II) chloride and two Schiff base ligands derived from rimantadine and 5-chlorosalicylaldehyde/4-methoxysalicylaldehydes, generated two novel complexes $[Zn(L^1)_2Cl_2]$ (**I**) and $[Zn(L^2)_2Cl_2]$ (**II**), where L^1 = 2-((1-(1-adamantan-1-yl)ethyl)-iminomethyl)-4-chlorophenol, L^2 = 2-((1-(1-adamantan-1-yl)ethyl)iminomethyl)-5-methoxyphenol. The complexes were characterized by the means of IR, ^1H NMR, elemental analysis, molar conductance and thermal analysis. A single-crystal X-ray diffraction analysis reveals that both complexes crystallize in orthorhombic system, space group *Fdd2* for **I** and *Pbcn* for **II**. In two complexes crystals, each asymmetric unit consists of one zinc(II) ion, two corresponding Schiff base ligands and two chlorine atoms; the central zinc atom lies on a twofold rotation axis and is four-coordinate via two chlorine atoms and two oxygen atoms from the Schiff base ligands, forming a distorted tetrahedral geometry.

DOI: 10.1134/S1070328414050054

INTRODUCTION

The field of Schiff base complexes attracts interest mainly due to facile synthesis and biological activity [1–4]. The diverse structures for the ligands rest with the types of aldehydes and amines [5]. Although obtained ligands involve in a broad scope such as single, double, asymmetric and macrocyclic Schiff bases, etc., the biological activity study of rimantadine-salicylaldehyde (or substituted salicylaldehyde) Schiff bases and their corresponding complexes has not been reported in detail [6].

The clinic medical research indicated that both amantadine (Symmetrel™) and rimantadine (Flumadine™) could block the ion channel formed by the M2 protein of influenza A viruses, result in inhibiting the early stages of virus replication. Therefore in many countries, amantadine and rimantadine have been widely used to treat or prevent seasonal influenza as efficacious remedies [7–10]. However, the incidence of side effects to central-nervous-system was higher with amantadine [11]. Salicylaldehyde and its derivatives are with antibacterial and antiviral activity and they were used to produce efficient herbicides, insecticides and fungicides [12]. Zinc is a vital element in the life for its taking part in a particular metabolic process [13, 14]. The Zn(II) complexes with Schiff bases were also found to be with biological activity and they demonstrated enhanced activities as compared to their parental ligands [15, 16]. In view of these points above, we designed and managed to synthesize a series of complexes containing both metal zinc(II) ion and the ligands derived from rimantadine and substituted salicylaldehyde. We hoped these zinc complexes could exhibit an extraordinary biological activity. In this work, two four-coordinate zinc(II) complexes $[Zn(L^1)_2Cl_2]$ (**I**) and $[Zn(L^2)_2Cl_2]$ (**II**), where L^1 = 2-((1-(1-adamantan-1-yl)ethyl)-iminomethyl)-4-chlorophenol, L^2 = 2-((1-(1-adamantan-1-yl)ethyl)iminomethyl)-5-me-thoxyphenol, were reported. Their absolute structures were determined by a single-crystal X-ray diffraction analysis. The antibacterial activities of two Schiff base ligands and their complexes against two bacteria of *Escherichia coli* and *Bacillus subtilis* were synchronously investigated.

EXPERIMENTAL

Materials and methods. All chemicals and solvents were of analytical grade and used as received. Elemental analysis was carried out on PerkinElmer Flash EA 1112.

[1] The article is published in the original.

Chemical shifts (**δ**) for ^{1}H NMR spectra were recorded at 300 MHz on a Varian Mercury-Vx300 spectrometer in $CDCl_3$ solvent containing TMS as an internal standard. Infrared spectrum (IR) was scanned in the range 4000 to 400 cm^{-1} with KBr pellets on a Nicolet NEXUS FT-IR 5700 spectrophotometer. Melting points were measured on a WRS-1B micro melting point apparatus which were uncorrected. The molar conductance of the complexes in DMF (1.0×10^{-3} mol L^{-1}) was measured on a DDS-11A conductormeter.

Synthesis of ligands. Two Schiff base ligands, 2-((1-(1-adamantan-1-yl)ethyl)-imino-methyl)-4-chlorophenol (**L^1**) and 2-((1-(1-adamantan-1-yl)ethyl)iminomethyl)-5-methoxyphenol (**L^2**), were prepared analogously to the literatures [17–20]. The synthetic route in this work was shown below:

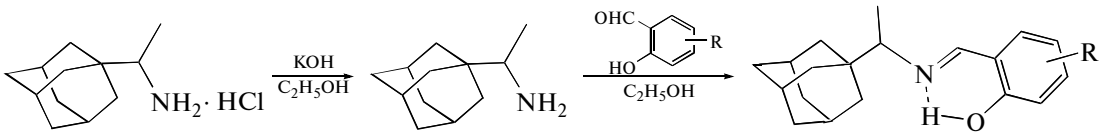

L^1: R = 4-Cl; L^2: R = 5-OCH_3

Rimantadine hydrochloride (3.0 mmol) and KOH (3.0 mmol) in 50 mL anhydrous alcohol were stirred for 24 h. The produced white precipitates (KCl) were filtered out and the transparent liquid was added dropwise to aldehyde (3.0 mmol) in 30 mL anhydrous alcohol under constant stirring. The resulting solution was refluxed for ~4 h, concentrated to about 20 mL through reduced pressure distillation and then stood at room temperature. A yellow solid appeared after 2–3 days with the solvent evaporation. The solid was filtered off and washed with anhydrous alcohol three times and air-dried.

Syntheses of the complexes. Zinc(II) chloride (1.0 mmol) in 20 mL anhydrous alcohol was added dropwise to a hot solution of a Schiff base ligand (1.0 mmol) in 20 mL anhydrous alcohol. Thereafter the mixture was refluxed for about 2 h and then kept at room temperature for overnight and complex precipitates were filtered off and dried. The yields were 58% for **I** and 62% for **II**.

For $C_{38}H_{48}N_2O_2Cl_4Zn$ (**I**) (M = 771.99)

anal. calcd., %:	C, 59.12;	H, 6.27;	N, 3.63.
Found, %:	C, 58.97;	H, 6.16;	N, 3.51.

For $C_{40}H_{54}N_2O_4Cl_2Zn$ (**II**) (M = 763.15)

anal. calcd., %:	C, 62.95;	H, 7.13;	N, 3.67.
Found, %:	C, 62.70;	H, 6.89;	N, 3.63.

The molar conductance values (Λ_M) are 6.10 and 8.64 S cm^2 mol^{-1} for **I** and **II**, respectively, which belong to the complex type of non-electrolytes molecular [17].

X-ray structure determination. Suitable crystals of **I** and **II** were grown by slow solvent evaporation of anhydrous alcohol. Diffraction data were collected on a Bruker Smart Apex II CCD with graphite monochromated MoK_α radiation (λ = 0.71073 Å) at 298(2) K using the ω-scan technique. The data were integrated by using the SAINT program, which also corrected the intensities for Lorentz and polarization effect [18]. An empirical absorption correction was applied using the SADABS program [19]. The structures were solved by direct methods using the program SHELXS-97 and all non-hydrogen atoms were refined anisotropically on F^2 by the full-matrix least-squares technique using the SHELXL-97 crystallographic software package [20]. The hydrogen atoms were generated geometrically. All calculations were performed on a personal computer with the SHELXL-97 crystallographic software package. The details of the crystal parameters, data collection and refinement are summarized in Table 1. Selected bond lengths and angles with their estimated standard deviations are given in Table 2. The molecular structures, as shown in Fig. 1, were visualized by Diamond [21].

Supplementary material for complexes **I** and **II** has been deposited with the Cambridge Crystallographic Data Centre (nos. 886789 (**I**), 853684 (**II**); deposit@ccdc.cam.ac.uk or http://www.ccdc.cam.ac.uk).

RESULTS AND DISCUSSION

The main IR data for **I** and **II** are given in Table 3, wherein several main data for ligands are also provided for comparison. Broad and intensity absorptions at 3433–3449 cm^{-1} for ligands and complexes can be identified as ν(O–H) indicating that phenolic hydroxyls of ligands are not deprotonated when the complexes are formed. The strongest absorptions at 1632 and 1623 cm^{-1} for ligands as well as 1648 and 1643 cm^{-1} for the complexes are the characteristics of ν(C=N); in metal complexes these bands undergo upward shift by 15 and 20 cm^{-1}. The spectra of the ligands show strong bands at 1279 cm^{-1} for L^1 and 1221 cm^{-1} for L^2, which is fairly certain to ν(C–O). In the complexes, this vibration band occurs at slight lower frequency with 1235 cm^{-1} for **I** and with 1214 cm^{-1} for **II**. The absorptions at 483 and 496 cm^{-1} for **I** and **II** are attributed to ν(Zn–O), indicating that oxygens of the Schiff bases are coordinated to Zn.

Table 1. Crystal data and structure refinement information for compounds **I** and **II**

Parameter	Value	
	I	**II**
Formula weight	771.59	763.12
Crystal system	Orthorhombic	Orthorhombic
Space group	*Fdd2*	*Pbcn*
a, Å	15.5281(12)	13.2436(14)
b, Å	43.024(15)	12.3110(13)
c, Å	10.9346(13)	24.888(2)
Volume, Å^3	7305(3)	4057.8(7)
Z	8	4
ρ_{calcd}, mg/m^3	1.403	1.249
Absorption coefficient, mm^{-1}	1.001	0.777
F(000)	3232	1616
Crystal size, mm	0.40 × 0.30 × 0.20	0.40 × 0.37 × 0.24
θ Range for data collection, deg	2.37–23.08	3.35–23.12
Limiting indices	$-18 \le h \le 15$,	$-15 \le h \le 14$,
	$-50 \le k \le 49$,	$-14 \le k \le 11$,
	$-12 \le l \le 12$	$-29 \le l \le 29$
Reflections collected	7027	19265
Independent reflections (R_{int})	3096 (0.0269)	3584 (0.0497)
Data/restraints/parameters	3096/1/199	3584/0/224
Goodness-of-fit on F^2	1.070	1.020
Final *R* indices ($I > 2\sigma(I)$)*	$R_1 = 0.0405$, $wR_2 = 0.0839$	$R_1 = 0.0505$, $wR_2 = 0.01190$
R indices (all data)*	$R_1 = 0.0490$, $wR_2 = 0.0897$	$R_1 = 0.0930$, $wR_2 = 0.1491$
Absorption correction	Empirical	
Refinement method	Full-matrix least-squares on F^2	
$\Delta\rho_{max}/\Delta\rho_{min}$, *e* Å^{-3}	0.24/–0.19	0.49/–0.19

* $R_1 = S||F_o| - |F_c||/|F_o|$; $wR_2 = [Sw(F_o^2 - F_c^2)^2 / \Sigma w(F_o^2)^2]^{1/2}$.

^{1}H NMR data for **I** and **II** in $CDCl_3$ are given in Table 4, where the data for ligands are also provided for comparison. Singlet peaks at 14.46–12.74 ppm for ligands and complexes are assigned to the phenolic hydroxyl protons. Because of intramolecular hydrogen bond formation of –CH=N···HO–, they are observed in low field. Moreover, in this range, the presence of integrated 1H for complexes indicates that phenolic hydroxyls of ligands are not deprotonated when the complexes are formed. The preservations of phenolic hydroxyls also can be confirmed by the corresponding IR spectra. The peaks at 8.19–7.70 ppm are assigned to the –CH=N proton. The aromatic hydrogens are a set of multiplets in the range of 7.27–6.24 ppm. The CH and CH_2 groups from adamantane are identified in the range of 2.00–1.50 ppm.

In order to ensure the stability of complexes in presence of polar solvent, such as DMF, a ^{1}H NMR titration study was carried out by adding DMF into complexes (complexes : DMF = 1 : 0.2/0.4/0.6/0.8/1.0, molar ratio) in $CDCl_3$, respectively, indicates both the complexes were rather stable in solution of DMF during 24 h.

In each asymmetric unit of two complexes crystals **I** and **II**, zinc atom lies on a twofold rotation axis and is four-coordinated via two chlorine atoms and two oxygen atoms from the Schiff base ligands, forming a distorted tetrahedral geometry with the smallest angle of O(1)Zn(1)Cl(2*A*) 99.19(9)° for **I** and

Table 2. Selected bond length (Å) and angles (deg) in **I** and **II***

Bond	*d*, Å	Bond	*d*, Å	Bond	*d*, Å
		I			
Zn(1)–O(1)	1.974(3)	N(1)–C(7)	1.300(4)	O(1)–C(1)	1.312(5)
Zn(1)–Cl(1)	2.2273(13)	N(1)–C(9)	1.482(5)	Cl(1)–C(4)	1.731(2)
		II			
Zn(1)–O(1)	1.957(3)	N(1)–Cl(1)	1.283(6)	O(1)–C(3)	1.312(4)
Zn(1)–Cl(1)	2.2342(12)	N(1)–C(10)	1.462(6)	O(2)–C(5)	1.350(5)
Angle	ω, deg	Angle	ω, deg	Angle	ω, deg
		I			
$O(1)^{i}Zn(1)O(1)$	111.91(18)	C(7)N(1)C(9)	122.4(3)	N(1)C(9)C(8)	109.3(4)
$O(1)^{i}Zn(1)Cl(2)$	99.19(9)	N(1)C(7)C(6)	123.59(17)	N(1)C(9)C(10)	110.3(3)
O(1)Zn(1)Cl(2)	113.65(9)	O(1)C(1)C(2)	122.6(3)	C(1)O(1)Zn(1)	130.3(3)
$Cl(2)^{i}Zn(1)Cl(2)$	119.89(7)	O(1)C(1)C(6)	119.4(3)		
		II			
$O(1)^{i}Zn(1)O(1)$	92.84(17)	C(3)O(1)Zn(1)	130.9(3)	C(1)C(2)C(7)	119.3(4)
$O(1)^{i}Zn(1)Cl(1)$	113.88(9)	C(5)O(2)C(8)	118.4(4)	C(3)C(2)C(7)	118.5(4)
O(1)Zn(1)Cl(1)	109.08(9)	N(1)C(1)C(2)	125.6(4)	O(1)C(3)C(4)	122.8(3)
$Cl(1)^{i}Zn(1)Cl(1)$	115.89(7)	O(1)C(3)C(2)	122.2(4)	O(1)C(3)C(2)	118.5(4)
C(1)N(1)C(10)	127.4(5)				

* Symmetry code: ^{i} $-x, -y + 2, z$.

Table 3. Main IR data for ligands and complexes (cm^{-1})

Compound	ν(C=N)	ν(C–O)	ν(C–H)*	ν(O–H)	ν(M–O)
L^1	1632 m	1279 w	2849 m	3433 m	
I	1648 s	1235 m	2850 m	3449 w	483 w
L^2	1623 s	1221 s	2845 s	3435 w	
II	1643 s	1214 m	2849 m	3434 w	496 w

* Adamantane ring C–H.

O(1)Zn(1)O(1*A*) 92.84(17)° for **II**, the biggest angle of Cl(2*A*)Zn(1)Cl(2) 119.89(7)° for **I** and O(1)Zn(1)Cl(2*A*) 113.88(9)° for **II**. The two phenyl rings are in the intersecting planes with a dihedral angle of 45.1(3)° for **I** and 75.3(3)° for **II**. The shortest distances between two adamantanyl carbons from two ligands are C(11)–C(11*A*) 9.724 Å for **I** and C(12)–C(12*A*) 6.714 Å for **II**, indicating *trans*-coordination of two ligands to zinc (Fig. 1). They are structurally very similar to another zinc(II) complex reported in [6]. The crystal structures also involve strong O–H···N intramolecular hydrogen bonds between the imino N and phenol O atoms, which benefit to stabilize the complex structures. The distances of H···O and N···O are 1.98 and 2.628 Å for **I**, 1.92 and 2.590 Å for **II**. The hydrogen bond angles of O–H···N are 132° for **I** and 134° for **II**.

Complex **I** and **II** are found neither intermolecular hydrogen bonding nor π–π interactions existences in stacking. The complexes molecules are regularly arranged by weak van der Waals forces to construct a net structure containing adamantine cages (Figs. 2 and 3).

The thermal gravimetric analysis was carried out with a heating rate of 20°C min^{-1} in an argon atmosphere over a temperature range of 25–800°C. The TG–DTG curves of **I** and **II** are in Fig. 4. The quite similar thermal decomposition appearances for **I** and **II** were observed with roughly two stages. The starting decomposition and weight loss for two complexes were approximately 220°C and the second rapid weight loss stages took place at approximately 330°C. When the complexes were heated above 550°C, the residues were deduced as oxides.

Two Schiff bases ligands and their zinc complexes were studied against a gram positive and a gram negative bacterium by inhibition zone method [22]. The compounds were prepared with four concentrations of 1.0×10^{-1}, 1.0×10^{-2}, 1.0×10^{-3}, 1.0×10^{-4} mo1 L^{-1} in DMF. The diameters of inhibition zone were measured after 48 h and the results are presented in Table 5.

All the complexes demonstrated superior antibacterial activities against *Escherichia coli* and *Bacillus subtilis* comparing with the corresponding

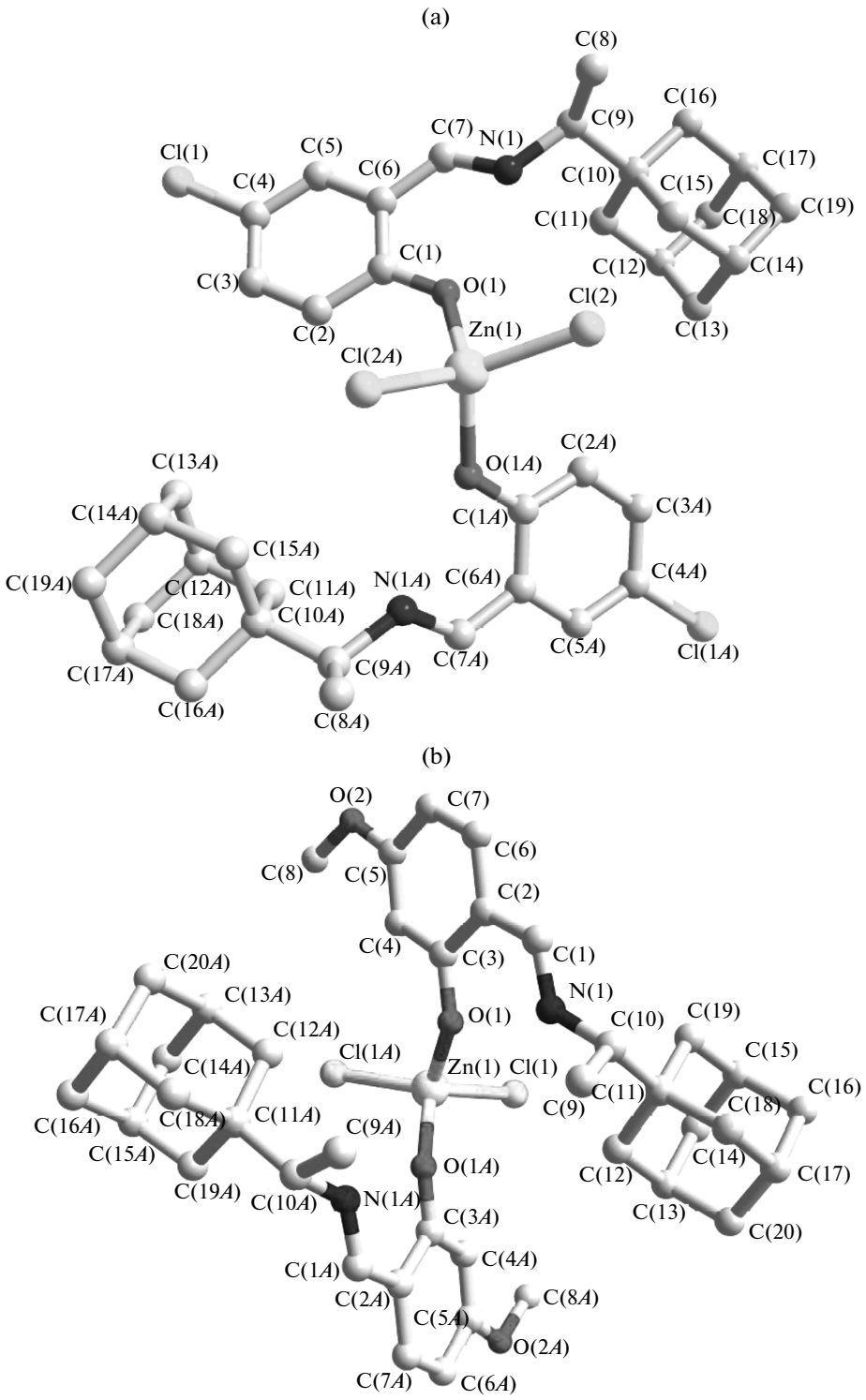

Fig. 1. X–ray structures of **I** (a) and **II** (b). Hydrogens are omitted for clarity.

ligands; the antibacterial ability of complexes was in a concentration-dependent. It is worth to note that complex **I** showed the maximum antibacterial effect against *Escherichia coli* and *Bacillus subtilis* in concentrated solution of 1.0×10^{-1} mo1 L^{-1}. In contrast with complexes, the two Schiff bases demonstrated inferior antibacterial activity under same testing conditions. Especially, L^1 was not found to have antibacterial ac-

Table 4. ^{1}H NMR data for ligands and complexes (δ, ppm; *J*, Hz)

Compound	Ar–OH	CH=N	Ar–H	Ar–OCH_3	N–CH	Adamantane ring–H	CH_3CH–N
L^1	13.93 (*s*, 1H)	8.19 (*s*, 1H)	7.26 (*d*, ^3J = 8.4, 1H); 7.22 (*s*, 1H); 6.90 (*d*, ^3J = 9.3, 1H)		2.86 (*q*, ^3J = 6.6, 1H)	1.99 (*s*, 3H, CH); 1.66 (*q*, ^3J = 12.3, 6H, CH_2); 1.54 (*d*, ^3J = 2.7, 6H, CH_2)	1.18 (*d*, ^3J = 6.6, 3H)
I	13.67 (*s*, 1H)	8.12 (*s*, 1H)	7.27 (*q*, ^3J = 9.0, 1H); 7.23 (*t*, ^4J = 2.1, 1H); 7.12 (*d*, ^3J = 9.0, 1H)		3.15 (*q*, ^3J = 5.7, 1H)	2.00 (*s*, 3H, CH); 1.66 (*q*, ^3J = 11.7, 6H, CH_2); 1.55 (*s*, 6H, CH_2)	1.32 (*d*, ^3J = 6.6, 3H)
L^2	14.46 (*s*, 1H)	8.01 (*s*, 1H)	7.06 (*d*, ^3J = 8.4, 1H); 6.37 (*s*, 1H); 6.32 (*d*, ^3J = 8.4, 1H)	3.79 (*s*, 3H)	2.82 (*q*, ^3J = 6.0, 1H)	1.97 (*s*, 3H, CH); 1.65 (*q*, ^3J = 12.0, 6H, CH_2); 1.53 (*s*, 6H, CH_2)	1.17 (*d*, ^3J = 6.3, 3H)
II	12.74 (*s*, 1H)	7.70 (*d*, ^3J = 12.9, 1H)	7.01 (*d*, ^3J =9.0, 1H); 6.93 (*s*, 1H); 6.24 (*dd*, ^3J = 9.0/8.7, 1H)	3.75 (*s*, 3H)	3.03 (*q*, ^3J = 6.6, 1H)	1.94 (*s*, 3H, CH); 1.60 (*q*, ^3J = 13.2, 6H, CH_2); 1.50 (*s*, 6H, CH_2)	1.28 (*d*, ^3J = 6.6, 3H)

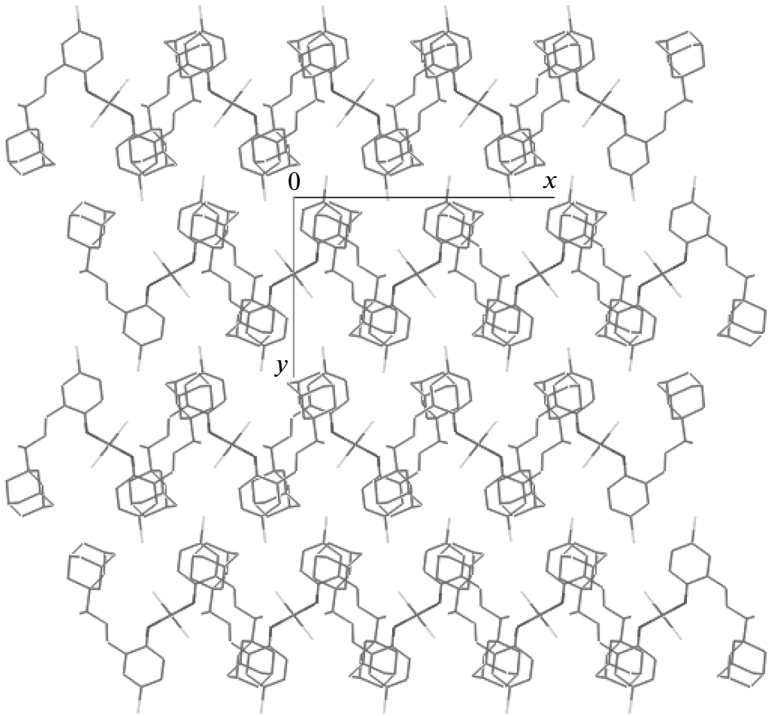

Fig. 2. The packing diagram of **I** viewed along the *z* axis.

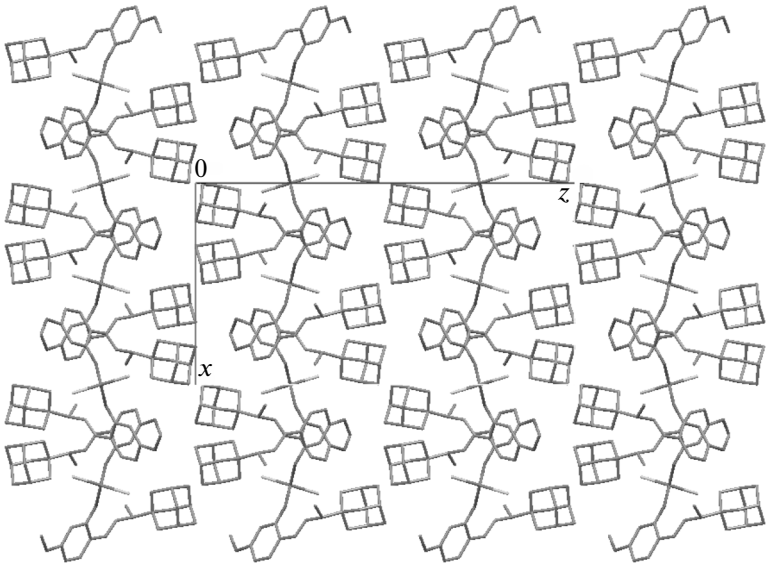

Fig. 3. The packing diagram of **II** viewed along the *y* axis.

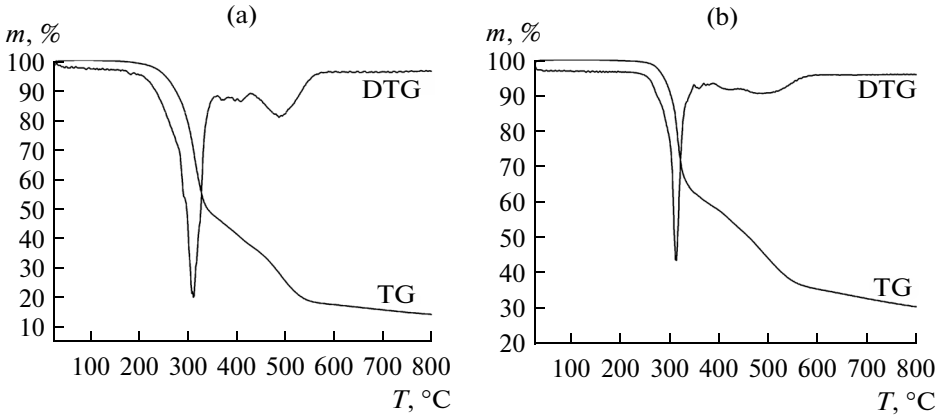

Fig. 4. The TG–DTG curves of complexes **I** (a) and **II** (b).

Table 5. Inhibitory of compounds against bacteria growth (inhibition zone*/mm)

Bacteria name	*Escherichia coli*				*Bacillus subtilis*			
Concentration (mol L^{-1})	1.0×10^{-1}	1.0×10^{-2}	1.0×10^{-3}	1.0×10^{-4}	1.0×10^{-1}	1.0×10^{-2}	1.0×10^{-3}	1.0×10^{-4}
L^1	8.5 ± 0.5	8.0	6.0 ± 0.5	6.0	6.0	6.0	6.0	6.0
I	15.5 ± 0.5	13.0 ± 0.5	9.0	7.5 ± 0.5	15.0	10.3 ± 0.5	7.0	6.0
L^2	7.7 ± 0.5	7.0	6.0	6.0	8.7 ± 0.5	8.3 ± 0.5	6.7 ± 0.5	6.7 ± 0.5
II	12.0	11.0	7.5 ± 0.5	6.0	16.0	11.3 ± 0.5	7.8 ± 0.5	6.0

* Filter paper diameter being 6.0 mm.

tivity against *Bacillus subtilis* at above mentioned concentrations.

ACKNOWLEDGMENTS

This work was financially supported by Foundation of Liaoning Provincial Department of Education Innovation Team Projects (LT2012001), the Cause of Public Welfare Scientific Research Fund (2012004001), Shenyang Science and Technology Plan Project (F13-289-1-00), Liaoning University Foundation of 211 Project for Innovative Talents Training and the Technology Major Projects Research Foundation (2011ZX09102-007-02), China.

REFERENCES

1. Zaki, Z.M., Haggag, S.S., and Soayed, A.A., *Spectrosc. Lett.*, 1998, vol. 31, no. 4, p. 757.
2. Chantarasiri, N., Ruangpornvisuti, V., Muangsin, N., et al., *J. Mol. Struct.*, 2004, vol. 701, nos. 1–3, p. 93.
3. Garnovskii, A.D., Nivorozhkin, A.L., and Minkin, V.I., *Coord. Chem. Rev.*, 1993, vol. 126, no. 1, p. 1.
4. Jin, X.D., Jin, Y.H., Zou, Z.Y., et al., *J. Coord. Chem.*, 2011, vol. 64, no. 9, p. 1533.
5. Mohamed, G.G. and Abd El-Wahab, Z.H., *J. Therm. Anal. Cal.*, 2003, vol. 73, no. 1, p. 347.
6. Zhao, G.L., Feng, Y.L., and Liu, X.H., *Chin. J. Inorg. Chem.*, 2005, vol. 21, no. 4, p. 598.
7. Pielak, R.M. and Chou, J.J., *Protein Cell*, 2010, vol. 1, no. 3, p. 246.
8. Tsunoda, A., Maassab, H.F., Cochran, K.W., and Eveland, W.C., *Antimicrob. Agents Chemother.*, 1965, vol. 5, p. 553.
9. Hayden, F.G., Minocha, A., Spyker, D.A., and Hoffman, H.E., *Antimicrob. Agents Chemother.*, 1985, vol. 28, no. 2, p. 216.
10. Schroeder, C., Heider, H., Möncke-Buchner, E., and Lin, T., *Eur. Biophys. J.*, 2005, vol. 34, no. 1, p. 52.
11. Dolin, R., Reichman, R.C., Madore, H.P., et al., *Engl. J. Med.*, 1982, vol. 307, no. 10, p. 580.
12. Hodnett, E.M. and Dunn, W.J., *J. Med. Chem.*, 1970, vol. 13, no. 4, p. 768.
13. Naumann, C.F., Prijs, B., and Sigel, H., *Eur. J. Biochem.*, 1974, vol. 41, no. 2, p. 209.
14. Burley, S.K., David, P.R., Sweet, R.M., et al., *J. Mol. Biol.*, 1992, vol. 224, no. 1, p. 133.
15. Singh, A.K., Pandey, O.P., and Sengupta, S.K., *Spectrochim. Acta*, *A*, 2012, vol. 85, no. 1, p. 1.
16. Singh, K., Barwa, M.S., and Tyagi, P., *Eur. J. Med. Chem.*, 2007, vol. 42, no. 3, p. 394.
17. Geary, W.J., *Coord. Chem. Rev.*, 1971, vol. 7, no. 1, p. 81.
18. *Bruker. SAINT, Version 6.02a*, Madison (WI, USA): Bruker AXS Inc., 2002.
19. Sheldrick, G.M., *SADABS*, *Program for Bruker Area Detector Absorption Correction*, Göttingen (Germany): Univ. of Göttingen, 1997.
20. Sheldrick, G.M., *SHELXS-97*, *Program for the Refinement of Crystal Structures*, Göttingen (Germany): Univ. of Göttingen, 1997.
21. Brandenburg, K., *Diamond*, *Version 3.2q*, Bonn (Germany): Crystal Impact GbR, 2011.
22. Bauer, A.W., Kirby, W.M.M., Sherris, J.C., and Turck, M., *Am. J. Clin. Pathol.*, 1966, vol. 45, no. 4, p. 493.